Improvement of the Starting and Braking Times of an Induction Motor Including Magnetic Saturation

Djamal Aouzellag, Kaci Ghedamsi, Hocine Amimeur and Saci Taraft

***Abstract*— Within this present paper, an optimization method for the starting and braking times of the induction cage motor including magnetic saturation is proposed. This method allows us to start or to brake the motor with a raised electromagnetic torque and a limited current so as to enhance the starting or braking times. This method uses Lagrange optimization to solve a constrained problem that is: while keeping the current limited, get the maximum torque at each time. The principle of this method is presented and the possibility to regulate the speed is also proposed. At last, simulation results justify the fidelity of this method.**

***Index Terms*— Constrained Optimization, Induction Motor, Saturation, Speed Regulation, Starting and Braking Times.**

I. Introduction

IN the field of driving at variable speed, the induction motor (IM) is usually used, for its robustness and it's relatively low cost. But this motor has a problem at starting because the electromagnetic torque developed by the machine is relatively weak compared to the called current [1] - [3].

Various modes of starting of IM were applied for various applications, that is to say by improving the electromagnetic torque with the detriment of an important current or the reverse.

The present paper is dedicated to the elaboration of an original technique to optimize properties of electromechanical devices and controlled systems taking in consideration for multiple requirements and restraining conditions. In particular, we have designed a new method to minimize availability time interval of induction motors at accelerated amplitude-frequency start or brake and a given set of current limitations including magnetic saturation.

In this paper, we present firstly, the static model of induction motor including saturation of the iron curve; then we expose the principle of the optimization method of the time starting/time braking based on the Lagrange optimization [1]. Secondly, the dynamic model of induction motor is presented as well as the experimental measures to determine the magnetic characteristic. Thirdly, we propose the cascade two-rectifier-three levels NPC PWM inverter [4] - [5]. The references values of frequency and ratio voltage of this converter are calculated using our optimization method. Finally, the system shown in Fig. 1 is used for numerical simulation and the related results are presented.

D. Aouzellag, K. Ghedamsi and S. Taraft are with Electrical Engineering Department, A. Mira University, Bejaia, Algeria (e-mail: aouzellag@hotmail.com; kghedamsi@yahoo.fr).

H. Amimeur was with LEB-Research Laboratory, Department of Electrical Engineering, University of Batna. Street Chahid Mohamed El hadi Boukhlouf, 05000, Batna, Algeria (e-mail: amimeurhocine2002@yahoo.fr.)

II. Induction Machine Static Modeling

Using the static model of induction machine in equivalent T diagram [6] - [7]; the different impedances are defined as follows:

$Z_s = \sqrt{R_s^2 + (A.X_s)^2}$: stator impedance module;

$Z'_r = \sqrt{(R_s/s)^2 + (A.X'_r)^2}$: rotor impedance module brought back to the stator.

It is considered that the magnetic losses are proportional to the frequency, which makes it possible to write:

$Z_m = A.\sqrt{R_m^2 + X_m^2}$: magnetizing circuit impedance module.

X_s, X'_r, R_m and X_m: the parameters of the motor.

They are calculated for the rated frequency f_{nom}. The magnetic circuit saturation is function of the electro motion force, i.e. $X_m = \varphi(E_1)$.

The multiplying factor A, with witch one varies the frequency f, compared to the f_{nom}, is defined as follow: $A = f/f_{nom}$.

The equivalent impedance using T diagram $\underline{Z}_{eq}$ is defined by: $\underline{Z}_{eq} = \underline{Z}_s + \underline{Z}_o$.

With:

$$\underline{Z}_o = \frac{\underline{Z}'_r.\underline{Z}_m}{\underline{Z}'_r + \underline{Z}_m}.$$

The e.m.f is defined by stator frequency, as follows: $E = AE_1$.

The expression of the electromagnetic torque:

$$T_e = \frac{P_{em}}{\Omega_s} = \frac{m.p.I'^2_r.\frac{R'_r}{s}}{2.\pi.f} = \frac{m.p.E^2.\frac{R'_r}{s}}{2.\pi.f.Z'^2_r} \qquad (1)$$

With m: the number of phases, p: the pole-pairs number and the synchronous angular speed: $\Omega_s = \frac{2\pi f}{p}$.

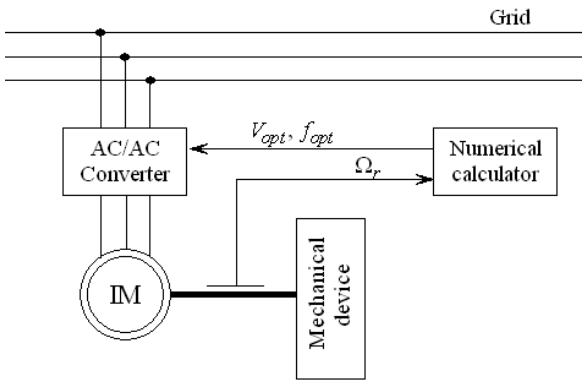

Fig. 1. Scheme of the studied device.

III. Starting or Braking Current Limitation with Taking into Account Saturation

A. Principle of the Method

By applying the Lagrange method to solve our problem, there will be the function to optimize and two constraints [1], [8]:

$$F_1 = T_e + \lambda_1(I_s^2 - I_{lim}^2) + \lambda_2(X_m - \varphi(E_1)) \quad (2)$$

With $T_e = f(s, E_1, X_m)$: electromagnetic torque;
$G_1(s, E_1, X_m) = (I_s^2 - I_{lim}^2) = (\frac{A.E_1}{Z_o})^2 - I_{lim}^2 = 0$ and $G_2(E_1, X_m) = X_m - \varphi(E_1) = 0$: two constraints;
λ_1, λ_2: Lagrange multipliers.

For each value of the frequency, one seeks to optimize the electromagnetic torque with keeping statoric current close to the limiting current I_{lim}. Moreover, the motor saturation is included.

For the first condition, the limit current (I_{lim}) is defined as follows: $I_{lim} = k.I_{nom}$ (k is a multiplying factor).

For the second condition, saturation of the magnetic circuit is added. The reactance X_m is a polynomial function of the e.m.f E_1:

$$X_m = \varphi(E_1) = \sum_{i=0}^{n} a_i E_1^i \quad (3)$$

With a, n: coefficients and degree of the polynomial.

B. Application of the Method to Limit the Starting or Braking Current

By applying the Lagrange algorithm for our problem, the system of five equations and five variables is obtained for each frequency f = Constant, as follows:

$$\frac{dT_e}{ds} + \lambda_1 \frac{d}{ds}(I_s^2 - I_{lim}^2) + \lambda_2 \frac{d}{ds}(X_m - \varphi(E_1)) = 0 \quad (4)$$

$$\frac{dT_e}{dE_1} + \lambda_1 \frac{d}{dE_1}(I_s^2 - I_{lim}^2) + \lambda_2 \frac{d}{dE_1}(X_m - \varphi(E_1)) = 0 \quad (5)$$

$$\frac{dT_e}{dX_m} + \lambda_1 \frac{d}{dX_m}(I_s^2 - I_{lim}^2) + \lambda_2 \frac{d}{dX_m}(X_m - \varphi(E_1)) = 0 \quad (6)$$

$$I_s^2 - I_{lim}^2 = 0; \qquad X_m - \varphi(E_1) = 0 \quad (7)$$

Arranged the system (4)-(7), we obtained another system (9)-(11) of three equations and three variables, with:

$$X'_m = \frac{\partial X_m}{\partial E_1} = \sum_{i=1}^{n} i a_i E_1^{i-1} \quad (8)$$

$$(R_m^2 + X_m^2)\begin{bmatrix} -(\frac{R'_r}{As})^4 + (R_m^2 + X_m^2 + 2X_m X'_r)(\frac{R'_r}{As})^2 \\ +X_r'^2(R_m^2 + (X'_r + X_m)^2) \end{bmatrix}$$
$$+E_1 X'_m((\frac{R'_r}{As})^2 - X_r'^2)\begin{bmatrix} -X_m(\frac{R'_r}{As})^2 + 2R_m X_m(\frac{R'_r}{As}) \\ +X'_r(X_m^2 - R_m^2 + X'_r X_m \end{bmatrix} = 0 \quad (9)$$

$$(\frac{AE_1}{Z_o})^2 - I_{lim}^2 = 0 \quad (10)$$

$$X_m - \sum_{i=0}^{n} a_i E_1^i = 0 \quad (11)$$

The resolution of the system of the equations (9)-(11) gives us four solutions, two real roots and two combined roots. The only roots to be considered are the real ones. The positive root as solution during starting and the negative root as solution during braking. Those roots, solution of this system for each frequency f value, are: E_{1_opt} and two values of the slip optimal s_{opt}, the positive value for starting and the negative value for braking.

The optimal angular speed is defined as follows:

$$\Omega_{r\_opt} = \frac{2\pi f_{nom} A}{p}(1 - s_{opt}) \quad (12)$$

- The optimum slips, at the beginning and the finishing of the starting ($\Omega_{r\_opt} = 0$ and $\Omega_{r\_opt} = \Omega_{r\_nom}$), are: $s_{opt} = 1$ and $s_{opt} = s_{nom}$.
- The optimum slips, at the beginning and the finishing of the braking ($\Omega_{r\_opt} = \Omega_{r\_nom}$ and $\Omega_{r\_opt} = 0$), are: $s_{opt} = -s_{nom}$ and $s_{opt} = 1$.

The optimal starting or braking times is defined as follows:

$$t_{opt} = \int_0^{\Omega_{r\_nom}} \frac{J}{T_{e\_opt} - T_r} d\Omega_{r\_opt} \quad (13)$$

Where J: total inertia;
$T_r = \frac{T_n}{\Omega_{r\_nom}}.\Omega_{r\_opt}$: torque resist.

For various values of the multiplying factor k, the solution of the problem is given in TABLE I.

IV. Experimental Measures

The experimental results have been performed in motor drives at no load, in order to determine the evolution of the magnetizing current with respects to the applied voltage per phase and adjusted the synchronism speed value to take the slip value null is to equivalent current rotor must be null, the induction motor is entrained by the synchronous motor with same pole pairs. Then, from these data and the used the static equivalent model of the motor drives, one can establish the evolution of the e.m.f E_1 per phase and magnetizing impedance X_m in function of magnetizing current I_m. The obtained curves are drawn in Fig. 2.

TABLE I
The Obtained Result with Optimization

Optimal value	Deferent value of multiplying factor k		
	0.75	1.0	2.0
Reactance of the magnetizing circuit AX_{m_opt} (Ω)	$22.39 \times A$	$20.4 \times A$	$16.95 \times A$
Slip s_{opt}	$\pm 0.014/A$	$\pm 0.019/A$	$\pm 0.038/A$
E.m.f $E_{opt} = AE_{1\_opt}(V)$	$247.2 \times A$	$257.7 \times A$	$268.5 \times A$
Magnetizing current $I_m(A)$	11.04	12.58	15.84
Rotor current $I'_r(A)$	17.93	24.99	52.11
Rotor current frequency $f_{r\_opt}(Hz)$	0.71	0.95	1.94
Ratio $E_{opt}/f_{opt}(V/Hz)$	4.94	5.15	5.37
Electromagnetic torque $T_{e\_opt}(N.m)$	± 42.48	± 61.23	± 134.54
Time starting $t_{opt}(s)$	35.50	10.50	2.75
Time braking $t_{opt}(s)$	4.75	3.63	1.90

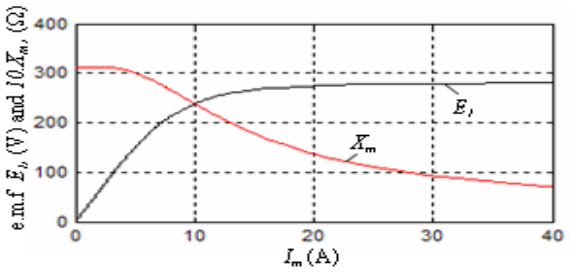

Fig. 2. E.m.f E_1 and X_m function to magnetizing current I_m.

V. Dynamic Model of the Induction Motor

In Park frame associated to the stator, the dynamic model of the IM taking into account the saturation is given by [1], [9] and [10]:

$$\begin{bmatrix} v_{ds} \\ v_{qs} \\ 0 \\ 0 \end{bmatrix} = \begin{bmatrix} R_s & -\omega_r \ell_s & 0 & -\omega_r L_m \\ \omega_r \ell_s & R_s & \omega_r L_m & 0 \\ -R_r & 0 & R_r & 0 \\ 0 & -R_r & 0 & R_r \end{bmatrix} \begin{bmatrix} i_{ds} \\ i_{qs} \\ i_{do} \\ i_{qo} \end{bmatrix} + \begin{bmatrix} \ell_s & 0 & L_m + L'_m \frac{i_{d0}^2}{i_o} & L'_m \frac{i_{d0} i_{q0}}{i_o} \\ 0 & \ell_s & L'_m \frac{i_{d0} i_{q0}}{i_o} & L_m + L'_m \frac{i_{q0}^2}{i_o} \\ -\ell_r & 0 & \ell_r + L_m + L'_m \frac{i_{d0}^2}{i_o} & L'_m \frac{i_{d0} i_{q0}}{i_o} \\ 0 & -\ell_r & L'_m \frac{i_{d0} i_{q0}}{i_o} & \ell_r + L_m + L'_m \frac{i_{q0}^2}{i_o} \end{bmatrix} \begin{bmatrix} \frac{di_{ds}}{dt} \\ \frac{di_{qs}}{dt} \\ \frac{di_{do}}{dt} \\ \frac{di_{qo}}{dt} \end{bmatrix} \quad (14)$$

With: $\omega_r = p\Omega_r$;
$L_m = \phi(i_o) = \sum_{j=0}^{n} b_j i_o^j$;
$L'_m = \frac{dL_m}{di_o} = \frac{d}{di_o}\phi(i_o) = \sum_{j=1}^{n} j b_j i_o^{(j-1)}$.
$i_o = \sqrt{i_{do}^2 + i_{qo}^2}$: current magnetizing module;
R_s, R_r: stator and rotor resistor;
$\ell_s = X_s/(2\pi f_{nom})$ and $\ell_r = X'_r/(2\pi f_{nom})$: leakage inductances;
$L_m = X_m/(2\pi f_{nom})$: inductance of magnetizing circuit.

The expression of the electromagnetic torque:

$$T_e = \frac{3}{2} p L_m (i_{do} i_{qs} - i_{qo} i_{ds}) \quad (15)$$

VI. Converter Modeling

The AC/AC converter (Fig. 1) consists of the cascade of two levels rectifier and three levels NPC PWM inverter (Fig. 3).

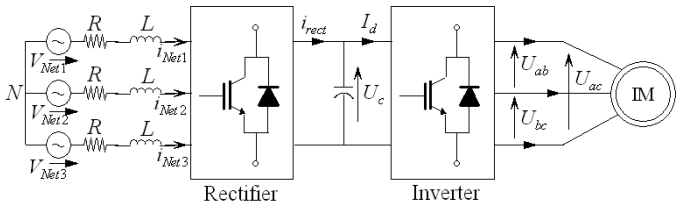

Fig. 3. Cascade two level rectifier-three level NPC PWM inverter.

A. Rectifier Model

A switching function G_{ij} is defined for each power switch (Fig. 4). It represents the ideal commutation orders and takes the values 1 when the switch is closed (on) and 0 when it is opened (off):

$$G_{ij} = \begin{cases} 1 & G_{ij} \text{ is closed} \\ 0 & G_{ij} \text{ is opened} \end{cases} \quad (16)$$

$i \in \{1,2,3\}$ n^o of the leg;
$j \in \{1,2\}$ n^o of the switch in the leg.

As ideal power switches are considered, the switches of a same leg are in complementary states:

$$G_{i1} + G_{i2} = 1, \qquad \forall i \in \{1,2,3\} \quad (17)$$

For both three-phase converters, modulation functions can be defined from the switching functions:

$$\underline{m} = \begin{bmatrix} m_{13} \\ m_{23} \end{bmatrix} = \begin{bmatrix} 1 & 0 & -1 \\ 0 & 1 & -1 \end{bmatrix} \cdot \begin{bmatrix} G_{11} \\ G_{21} \\ G_{31} \end{bmatrix} \quad (18)$$

The relation between the rectifier output-input voltages and currents is defined as below:

$$\begin{cases} V_{Net1} = \underline{m} U_c \\ i_{rect} = \underline{m}^t i_{Net1} \end{cases} \quad (19)$$

B. Modeling and Control of Three-Level NPC Source Voltage Inverter

Fig. 5 describes a three-level inverter structure.

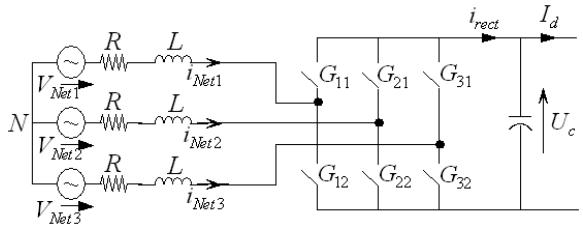

Fig. 4. Rectifier converter with ideals switches.

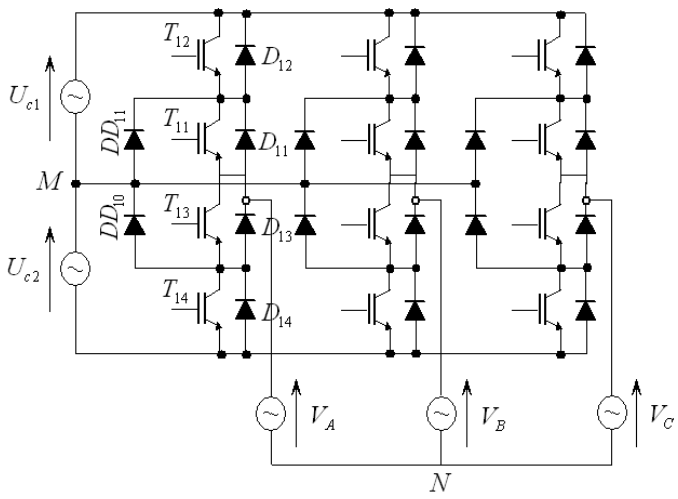

Fig. 5. The simple output voltage of the first arm, for $m = 9$, $r = 0.8$.

The simple output voltages are:

$$\begin{bmatrix} V_A \\ V_B \\ V_C \end{bmatrix} = \frac{U_c}{6} \begin{bmatrix} 2 & -1 & -1 \\ -1 & 2 & -1 \\ -1 & -1 & 2 \end{bmatrix} . \left\{ \begin{bmatrix} F_{11}^b \\ F_{21}^b \\ F_{31}^b \end{bmatrix} - \begin{bmatrix} F_{10}^b \\ F_{20}^b \\ F_{30}^b \end{bmatrix} \right\} \quad (20)$$

F_{k1}^b: connection functions of the upper half arm;
F_{k0}^b: connection functions of the lower half arm;
Where: $k = 1, 2, 3$.

C. Triangulo-Sinusoidal Strategy using Two Carriers

To use the characteristic that a three-level VSI is equivalent to two two-level VSI [4], [5]; and improve the spectrum characteristic of the inverter output, we propose to use two bipolar carriers (U_{P1}, U_{P0}) shifted each one from the other by half carrier period T_p. The algorithm of this strategy can be summarized in two steps:

Step1: determination of the intermediate signals (V_{k1}, V_{k0})

$$\begin{cases} V_{refk} \geq U_{p1} \Rightarrow V_{k1} = E/2 \\ V_{refk} < U_{p1} \Rightarrow V_{k1} = 0 \end{cases}$$

and:

$$\begin{cases} V_{refk} \geq U_{p0} \Rightarrow V_{k0} = 0 \\ V_{refk} < U_{p0} \Rightarrow V_{k0} = -E/2 \end{cases}$$

Step2: determination of the signal V_{k2} and the switch control order B_{ks}

$$\begin{cases} V_{k2} = E/2 \Rightarrow B_{k1} = 1, \quad B_{k2} = 1 \\ V_{k2} = -E/2 \Rightarrow B_{k1} = 0, \quad B_{k2} = 0 \\ V_{k2} = 0 \Rightarrow B_{k1} = 1, \quad B_{k2} = 0 \end{cases}$$

where:

$$\begin{cases} V_{k2} = V_{k1} + V_{k0} \\ B_{k3} = \overline{B}_{k2} \\ B_{k4} = \overline{B}_{k1} \end{cases} \quad \text{and} \quad k = 1, 2, 3.$$

Fig. 6 shows the simple output voltage of the first arm, for $m = 9$.

Fig. 7 shows the variations of the amplitude of the fundamental and the harmonics magnitude of the simple output voltage of a phase according to the modulation factor r, for $m = 9$.

VII. Results and Interpretation

In the first step, the AC/AC converter is supposed ideal. Fig. 8 shows the variation of f_{opt} and V_{opt} according to time. These variations are obtained by using the proposed optimization algorithm. The IM is connected to the grid via the ideal converter, in the first step. The stator current using static/dynamic model of the IM and the related expended plot are shown in Figs. 9 and 10. On the other hand, Fig. 11 gives the optimal electromagnetic torque and the resist torque. Fig. 12, in turn, shows the variation of the angular speed. Note that the different results using dynamic and static models of IM are almost the same.

In the second step, the cascade of rectifier-inverter is introduced. The references values, Fig. 13, (frequency and voltage ration) of the converter are obtained by using the proposed optimization algorithm. In this part, the possibility of speed regulation is devoted. The stator current and voltage and the related expended plot are show in Figs. 14, 15 and 16. Fig. 17 shows the optimal electromagnetic torque and the resist torque. The angular speed of the IM is plotted in Fig. 18. Fig. 19, in turn, shows the active and reactive powers.

For a possible confrontation of the results, the direct starting of the IM is operated without optimization. Fig. 20 shows the stator current and the angular speed. The electromagnetic and the resist torque are plotted in Fig. 21.

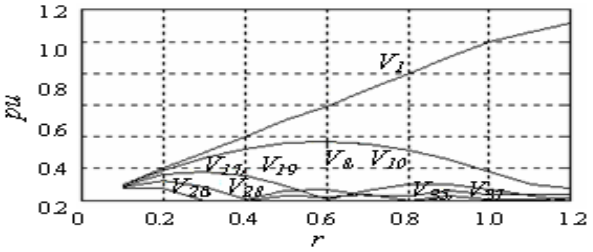

Fig. 7. The fundamental and the harmonics magnitude according r, for $m = 9$.

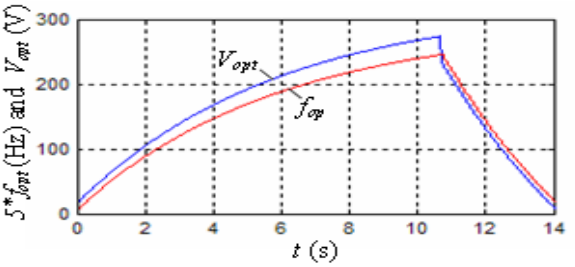

Fig. 8. Optimal frequency and voltage of stator.

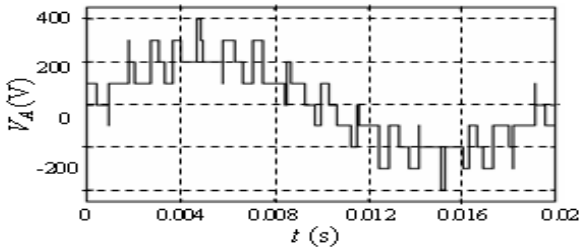

Fig. 6. The simple output voltage of the first arm, for $m = 9$, $r = 0.8$.

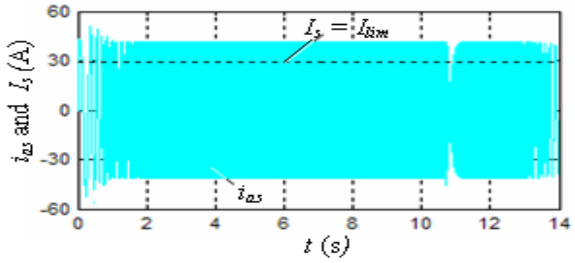

Fig. 9. Stator current.

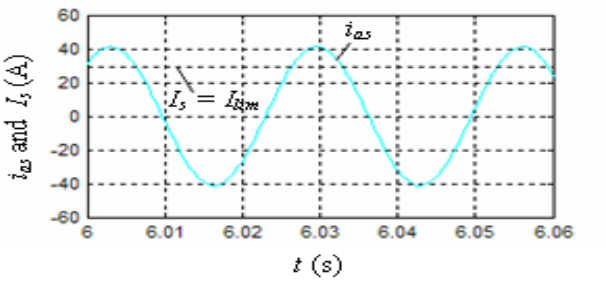

Fig. 10. Zoom of the stator current.

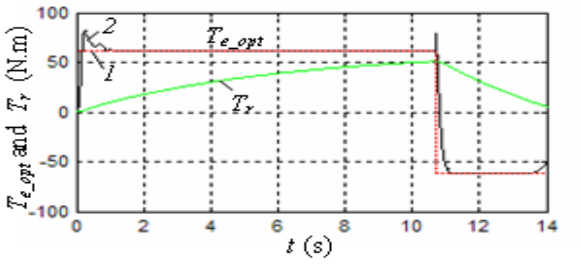

Fig. 11. Optimal electromagnetic and resist torque: 1- using static model; 2- using dynamic model.

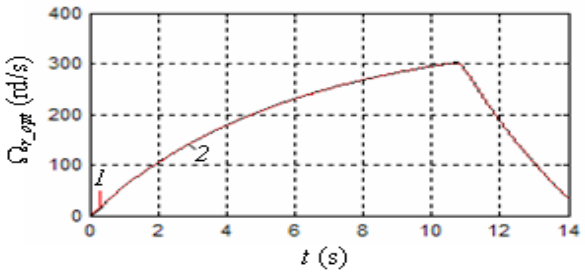

Fig. 12. Optimal rotor speed: 1- using static model; 2- using dynamic model.

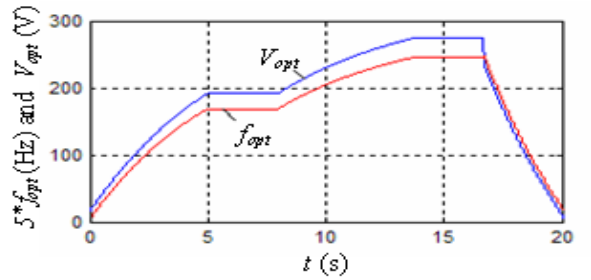

Fig. 13. Optimal reference frequency and voltage for the converter.

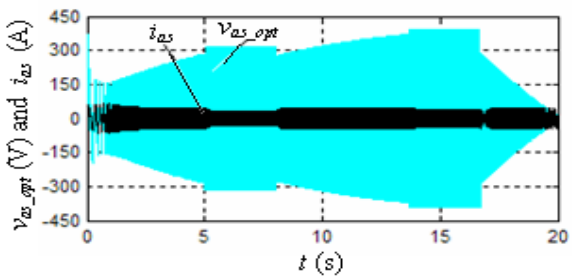

Fig. 14. Optimal voltage and current of stator.

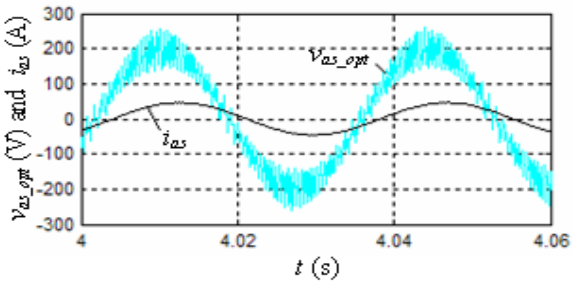

Fig. 15. Zoom of optimal voltage and current of stator.

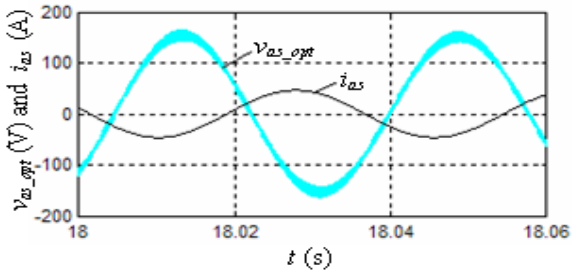

Fig. 16. Zoom of optimal voltage and current of stator.

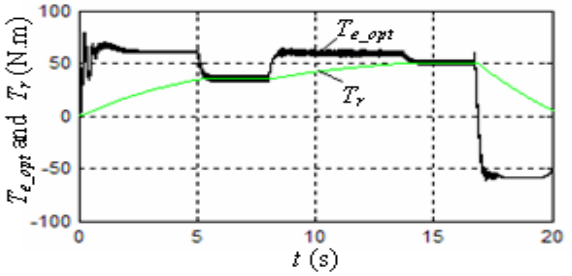

Fig. 17. Optimal electromagnetic torque and resist torque.

VIII. Conclusion

The optimization method exposed in this work, for starting or braking of an induction cage motor including magnetic saturation has the following advantages:

- reduction of the starting or braking times;
- the machine starts or brakes with a high electromagnetic torque;
- the call of the stator current is limited and constant then the losses can be reduced;
- the frequency and the amplitude of the rotoric currents remain constants during starting;
- the ratio E_{opt}/f_{opt} is constant, therefore flux is constant;
- the ratio V_{opt}/f_{opt} not constant for those lows values of frequency because the voltage drops to the stator.

IX. Machine Parameters

- Nominal voltage: $V_{nom} = 220V$;
- Nominal current: $I_{s\_nom} = 29A$;
- Electromagnetic torque: $T_{e\_nom} = 51.6N.m$;
- Stator resistor: $R_s = 0.402\Omega$;

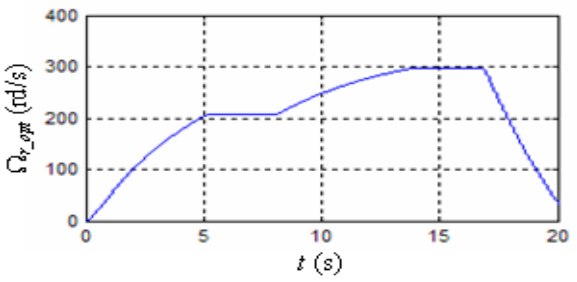

Fig. 18. Optimal rotor speed.

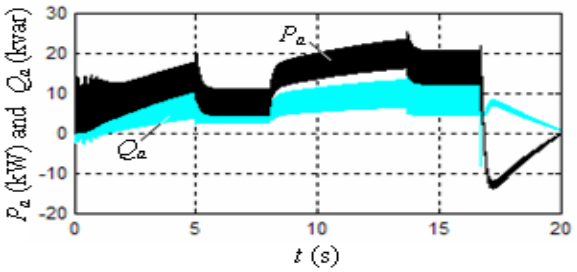

Fig. 19. Stator active and reactive powers.

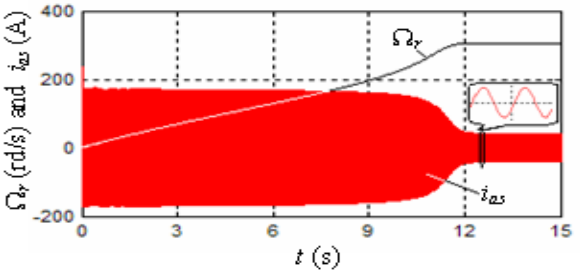

Fig. 20. Rotor speed and stator current.

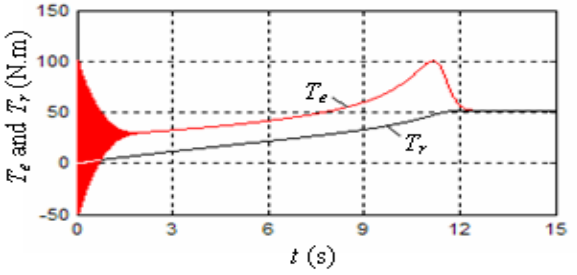

Fig. 21. Electromagnetic torque and resist torque.

- Rotor resistance brought back to the stator: $R'_r = 0.196\Omega$;
- Stator reactance: $X_s = 0.725\Omega$;
- Rotor reactance brought back to the stator: $X'_r = 1.02\Omega$;
- Magnetizing resistance: $R_m = 1.5\Omega$;
- Nominal slip: $s_n = 2.6\%$;
- Number of phases: $m = 3$;
- Number of pole pairs: $p = 1$;
- Total inertia: $J = 1kg.m^2$;

Note: The values of the various parameters are given to the rated frequency of $50Hz$.

REFERENCES

[1] D. Aouzellag, "Optimization of the frequency technical control for the induction electric actuators with the whole of fixed requirements and limitations," Ph.D. dissertation, National University of Aeronautics, Kiev, Ukraine, 2001.

[2] D. Aouzellag, A. Abaïche, K. Ghedamsi, "Minimization of the time of starting of an asynchronous cage motor with great inertia," 3^{rd} *International Conference on Electrical Engineering CEE'04*, University of Batna, Algeria, 2004.

[3] P. Caron, J. P. Hautier, "Modeling and ordering of the asynchronous machine," Editions Technip, Paris, 1995.

[4] K. Ghedamsi, "Modeling and realization of different strategy of drive the three-levels NPC inverter. Application to drive of the induction machine," Magister Works, EMP, Algeria, 2001.

[5] E. M. Berkouk, "Contribution to the drive of the single-phase and three-phase induction machines supplied with direct and indirect converters. Application to graduators and multi-levels inverters," Doctoral Thesis, C.N.A.M, 1995.

[6] M. P. Kostenko, L. M. Pitrovski, "Electrical Machines," Tome II, Energy, Moscow, 1973.

[7] F. Ben Ammar, "Variable speed transmission of high performances for induction machines of great power," Doctoral Thesis, I.N.P, Toulouse, 1993.

[8] G. Korn, T. Korn, "Mathematical handbook for scientists and engineers: definitions, theorems and formulas for reference and review," McGRAW-HILL Book Company, INC. New York Toronto London, 1961.

[9] K. Idjdarene, D. Rekioua, D. Aouzellag, "Modeling and simulation of wind conversion power system based on an induction generator taking the saturation into account," 3^{rd} *International Conference on Electrical Engineering CEE'04*, University of Batna, Algeria, 2004.

[10] D. Rekioua, K. Idjdarene, "An approach for the modeling of an autonomous induction generator taking into account the saturation effect," *International Journal of Emerging Electric Power Systems*, Volume 4, Issue 1, Article 1052, 2005.